

Green Chemistry: Sunlight-Induced Cationic Polymerization of Renewable Epoxy Monomers Under Air

Mohamad-Ali Tehfe,[†] Jacques Lalevée,^{*,†} Didier Gigmes,[‡] and Jean Pierre Fouassier[†]

[†]Department of Photochemistry, CNRS, University of Haute Alsace, Ecole Nationale Supérieure de Chimie de Mulhouse, 3 rue Alfred Werner, 68093 Mulhouse Cedex, France and [‡]UMR 6264 Laboratoire Chimie Provence, Université de Provence, Avenue Escadrille Normandie-Niemen, Case 542, Marseille 13397, Cedex 20, France

Received November 22, 2009; Revised Manuscript Received December 31, 2009

ABSTRACT: The recently developed silyl radical chemistry is used here for the free-radical-promoted cationic polymerization process (FRPCP) of two epoxy monomers (epoxidized soybean oil and limonene dioxide) that are representative of green monomers. The new developed photoinitiating systems are highly efficient under air upon a solar irradiation in autumn French weather and, for example, lead to 60% conversion after 25 min and form a completely tack-free and uncolored coating after 1 h. Polymerization profiles obtained upon a visible light irradiation delivered by a xenon lamp or a 405 nm diode laser under air show that 70% conversion can be easily achieved after 400 s of exposure. Excited-state processes are investigated and discussed.

Introduction

The use of natural products or renewable monomers for plastic materials has clearly become an important topic in polymer science. In the photopolymerization area, the development of systems that meet the demand of green chemistry with low energy requirement (or even with no energy using solar irradiation) is a matter of concern.^{1,2} For example, the cationic photopolymerization of epoxidized natural oils or products has been elegantly investigated in different previous studies.^{3–6} It has been particularly demonstrated that triglycerides can be transformed in epoxy monomers from plant oils by a chemical modification.^{3–6} In a general way, the plant oil derivatives present attractive features such as versatility, biodegradability, and low cost. Recently, a very interesting system based on curcumin as an electron transfer agent for the photosensitized decomposition of an iodonium hexafluoroantimonate has been developed for the cationic polymerization of epoxidized soybean or linseed oils in laminate under visible light and even sunlight.^{6b} Cationic photopolymerization under sunlight and particularly under an aerated atmosphere (contrary to laminate conditions) remains an important challenge.^{2b} The development of new initiating systems is still requested.

In this laboratory, we are interested in the design of systems that are able to polymerize efficiently radical or cationic monomers under air, upon visible light exposure, or both.^{7–9} Free-radical-promoted cationic polymerization process (FRPCP) has been recognized as an interesting method^{10–16} where radicals are produced from usual type I or type II radical photoinitiator (PI) and oxidized by a diaryliodonium salt, the resulting cations being the polymerization-initiating structures. FRPCP for visible light is the subject of many elegant works.^{6a,11,13,14,16} The drawback of FRPCP remains obviously the observed oxygen inhibition.^{2b,6a,11} Among the various proposed systems for FRPCP, polysilanes were mentioned 15 years ago as capable of initiating FRPCP processes in degassed solutions.¹² Our recent works based on the silyl radical chemistry have largely introduced new developments

for carrying out FRPCP in film under air and upon various light sources (Hg lamp, Xe–Hg lamp, LED, laser).^{7,8a,9}

The outstanding specificity of the silyl radical chemistry prompted us to investigate the photopolymerization of renewable monomers (epoxidized soybean oil (ESO) and limonene dioxide (LDO), see Scheme 1) under sunlight and under air in the presence of a radical source (mainly phosphineoxide derivatives), tris-(trimethylsilyl)silane (TTMSS), and diphenyl iodonium hexafluorophosphate. ESO is obtained by an epoxidation reaction of soybean oil. Limonene (or Dipentene) is a terpene liquid found in various volatile oils such as cardamon, nutmeg, and turpentine oil. LDO can be formed through oxidation of limonene with peracids. LDO that has been already encountered in many cationic photopolymerization processes⁶ is mainly used here as a reference. The design of new suitable systems sensitive under visible lights, the cationic photopolymerization of ESO and LDO under air and upon sunlight, the recording of the conversion–time profiles obtained upon a visible light irradiation delivered by a xenon lamp or a 405 nm diode laser under air, as well as the reactivity of the silylium cations will be presented. The mechanisms will be discussed using laser flash photolysis (LFP) and ESR spin trapping experiments (ESR-ST).

Experimental Part

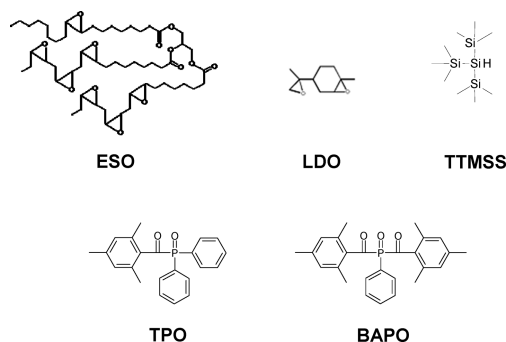
Compounds. The investigated compounds are shown in Scheme 1. TTMSS, isopropylthioxanthone (ITX), and diphenyl iodonium hexafluorophosphate (Ph₂I⁺) were obtained from Aldrich, and phenylbis(2,4,6-trimethylbenzoyl)phosphine oxide (BAPO) or 2,4,6-trimethylbenzoyl-diphenyl phosphine (TPO) were obtained from Ciba-Basel.

ESO was obtained from Arkema (Ecepoxy; epoxy content: 3.7 M/kg), and LDO was obtained from Millennium Specialty Chemicals. (3,4-Epoxy)cyclohexane)methyl 3,4-epoxycyclohexyl-carboxylate (EPOX, UVACURE 1500) was a gift of Cytec.

Free-Radical-Promoted Cationic Polymerization Processes. In FRPCP experiments, three different photoinitiating systems based on BAPO, TPO (1% w/w), or ITX (0.1% w/w) were studied. A weight concentration of 1% w/w in diphenyliodonium hexafluorophosphate (Ph₂I⁺) was added. TTMSS was

*Corresponding author. E-mail: j.lalevee@uha.fr.

Scheme 1



also used as an additive (3% w/w). The photoinitiating systems were: BAPO/TTMSS/Ph₂I⁺ (1/3/1% w/w), TPO/TTMSS/Ph₂I⁺ (1/3/1% w/w), or ITX/TTMSS/Ph₂I⁺ (0.1/3/1% w/w).

The films (25 μm thick) deposited on a BaF₂ pellet were irradiated with the polychromatic light (to ensure a visible light irradiation, a cut off filter has been used to select $\lambda > 390$ nm) of a Xenon lamp (Hamamatsu, L8253, 150 W; incident light intensity: $I_0 \approx 60 \text{ mW cm}^{-2}$ in the $390 < \lambda < 800$ nm range). Some monochromatic diode laser irradiations at 405 nm were also carried out (cube – continuum; $I_0 \approx 8 \text{ mW cm}^{-2}$). The evolution of the epoxy group content is continuously followed by real time FTIR spectroscopy (Nexus 870, Nicolet), as reported in refs 7–9. The absorbance of the epoxy group was monitored at $\sim 830 \text{ cm}^{-1}$. The Si–H conversion for TTMSS was followed at $\sim 2050 \text{ cm}^{-1}$. The sunlight exposure is described below.

Laser Flash Photolysis (LFP). The nanosecond laser flash photolysis LFP experiments were carried out with a Q-switched nanosecond Nd/YAG laser at $\lambda_{\text{exc}} = 355$ nm (9 ns pulses; energy reduced down to 10 mJ; Powerlite 9010 Continuum), the analyzing system consisting of a pulsed xenon lamp, a monochromator, a fast photomultiplier, and a transient digitizer.¹⁷

ESR Spin Trapping (ESR-ST) Experiments. ESR-ST experiments were carried out using a X-Band spectrometer (MS 200 Magnetech). The radicals were produced at RT under the exposure of a Xenon lamp and trapped by phenyl-*N*-tbutylnitron (PBN) according to a procedure described in detail in ref 18.

Results and Discussion

1. FRPCP of Renewable Monomers. *A. Sunlight Irradiation.* The solar irradiation was carried out under air and cloudy weather in October in Mulhouse (France); an absolute irradiance measurement (Ocean Optics HR4000) leads to an estimated incident energy $< 0.5 \text{ mW/cm}^2$ in the 390–420 nm range. An outdoor exposure of the sample for ~ 20 min was enough to obtain already a good polymerization result. For the systems based on BAPO/TTMSS/Ph₂I⁺ or TPO/TTMSS/Ph₂I⁺, completely tack-free coatings are obtained after 1 and 3 h for LDO and ESO, respectively. In the absence of TTMSS, the samples remain tacky. Figure 1 shows that an outdoor irradiation of 25 min leads to a conversion of $\sim 60\%$ for LDO using the TPO/TTMSS/Ph₂I⁺ system. A final conversion of $\sim 80\%$ is reached after 1 h, and the system is tack free. A concomitant increase in the band at $\sim 1080 \text{ cm}^{-1}$ is also observed because of the formation of the polyether. A strong bleaching of the TPO (or BAPO)/TTMSS/Ph₂I⁺ containing film during the irradiation is noted (Figure 1), leading to a colorless coating.

When using ITX/Ph₂I⁺, the addition of TTMSS leads to slightly better polymerization kinetics; that is, for a solar irradiation of 10 min (Figure 1B), the conversion of LDO is increased from 60 to 65%. Tack-free coatings are also

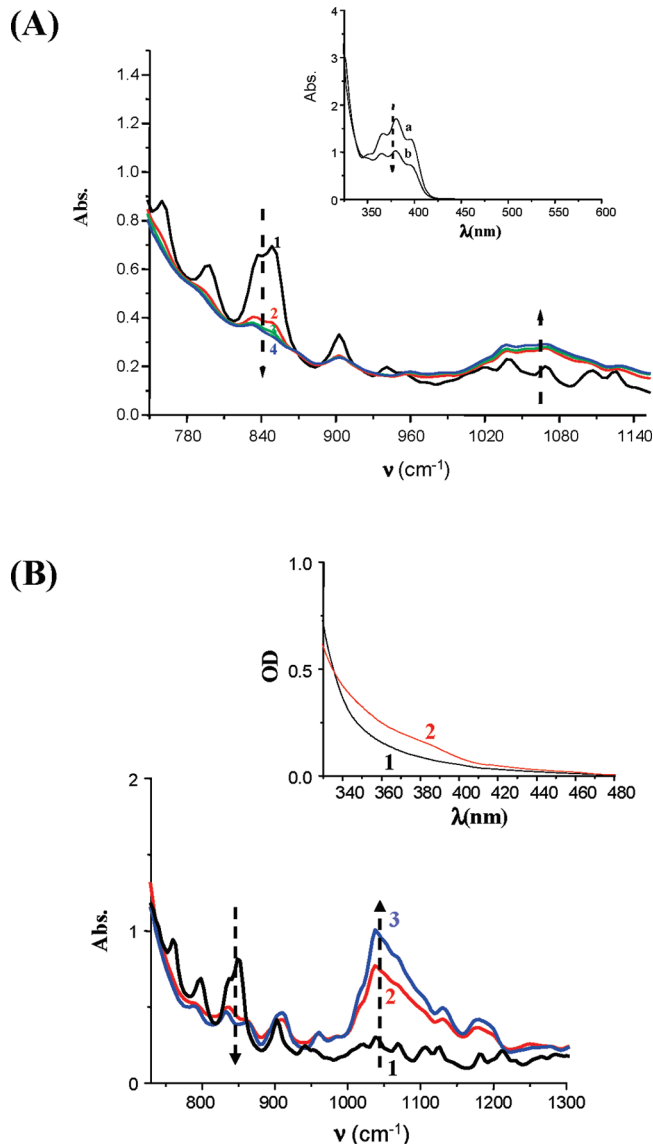


Figure 1. (A) IR spectra recorded during the photopolymerization of LDO under sunlight irradiation in the presence of the TPO/TTMSS/Ph₂I⁺ (1/3/1% w/w) photoinitiating system: $t = 0$ (1); $t = 25$ min (2); $t = 40$ min (3); and $t = 55$ min (4) (tack free). Insert: UV–visible absorption of a TPO/TTMSS/Ph₂I⁺-containing film (thickness 1 mm) during the irradiation: $t = 0$ (a) and $t = 5$ min (b). (B) IR spectra recorded during the photopolymerization of LDO under sunlight irradiation in the presence of the ITX/Ph₂I⁺ (1/1% w/w) for $t = 0$ (1); $t = 10$ min (2); and $t = 10$ min with the addition of TTMSS 3% w/w (3). Insert: UV–visible absorption spectra of a ITX/TTMSS/Ph₂I⁺-containing film (2) and a TPO/TTMSS/Ph₂I⁺-containing film (1) after sunlight irradiation.

obtained, for example, for LDO upon 20 and 25 min irradiations using ITX/TTMSS/Ph₂I⁺ (1/3/1% w/w) and ITX/Ph₂I⁺ alone (1/1% w/w), respectively. Contrary to the phosphine-oxide-based systems, the coating exhibits a detrimental yellowing (Figure 1B) that can be likely ascribed to an insufficient ITX consumption.

B. FRPCP under the Xenon Lamp and the Diode Laser (405 nm). As expected, when using BAPO/Ph₂I⁺, very low conversions are reached under air. The addition of TTMSS drastically improves the polymerization process for both the diode laser and the xenon lamp irradiations (Figures 2 and 3). A high conversion of the Si–H functions is also noted ($\sim 70\%$). For TPO, similar trends are observed; that is, the polymerization processes lead to significant conversion

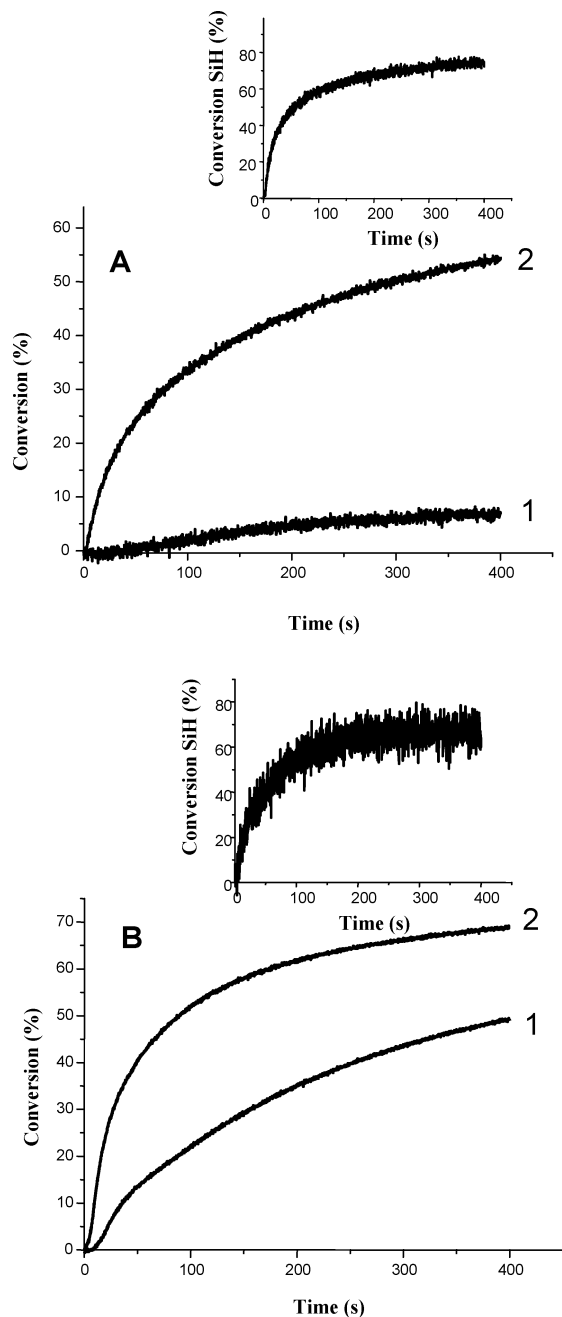


Figure 2. Polymerization profiles of (A) ESO and (B) LDO. Under air. Upon a diode laser irradiation (405 nm) in the presence of (1) BAPO/Ph₂I⁺ (1/1% w/w) and (2) BAPO/TTMSS/Ph₂I⁺ (1/3/1% w/w). Insert: conversion of the Si–H content in the case of (2).

under air only upon the addition of TTMSS (Figure 1 in the Supporting Information). Compared with TPO, BAPO leads to a slightly better conversion.

In contrast, as above, the well-known ITX/Ph₂I⁺ system allows an already quite efficient polymerization that is only slightly improved by the addition of TTMSS (Figure 4); a decrease in the inhibition time for the polymerization under air is mainly observed with TTMSS. Such a behavior has been previously observed for the FRPCP of usual epoxides.⁹ However, despite the low effect on the monomer conversion, a high Si–H consumption is noted (insert of Figure 4).

In the case of the diode laser and xenon lamp irradiations, the light intensities used here are quite low and almost similar: 8 and 6.7 mW cm^{−2}, respectively, in the 390–420 nm photoinitiator absorption range. (See Figure 2 of the

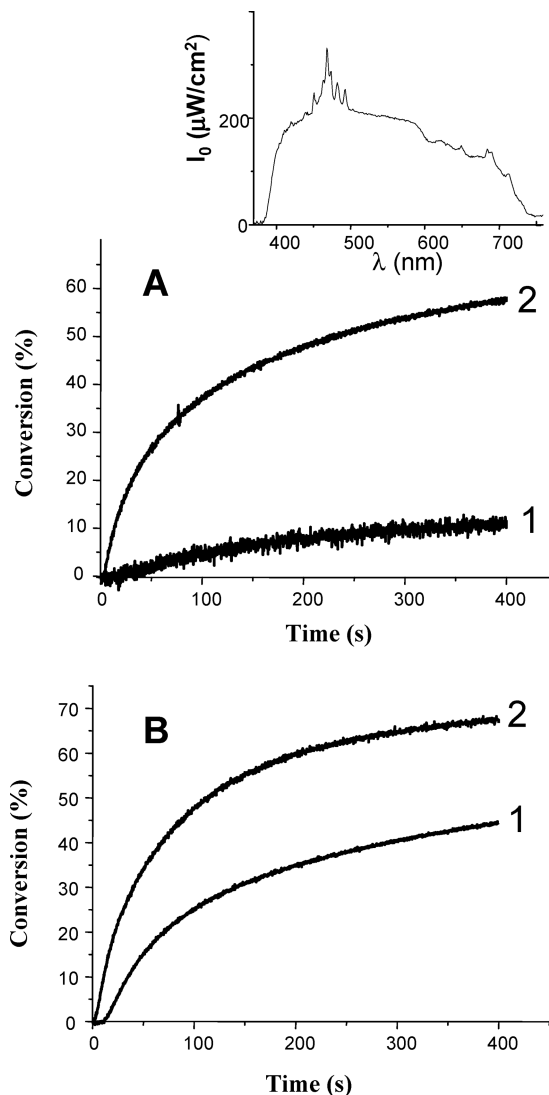


Figure 3. Polymerization profiles of (A) ESO and (B) LDO. Under air. Upon a Xenon lamp irradiation in the presence of (1) BAPO/Ph₂I⁺ (1/1% w/w) and (2) BAPO/TTMSS/Ph₂I⁺ (1/3/1% w/w). Insert: emission spectrum of the xenon lamp.

Supporting Information.) This is in agreement with the quite similar polymerization profiles obtained under these experimental irradiation conditions. For the experiments carried out with the xenon lamp, the amount of light absorbed by ITX (0.1%), BAPO (1%), and TPO (1%) is in a ratio 0.33:1:0.25 (Supporting Information; the absorption of TTMSS or Ph₂I⁺ can be neglected for λ > 320 nm). The procedure to determine the amount of light absorbed has been presented in detail in ref 7. This is in line with the better polymerization rates obtained with BAPO compared with TPO, but the quite low efficiency difference (Figures 2 and 3 and Figure 1 in the Supporting Information) suggests that TPO exhibits a higher intrinsic reactivity than BAPO. For ITX, the polymerization profiles are quite similar to those obtained using BAPO; this demonstrates that the initiation quantum yield in the presence of ITX is probably better. A similar trend is observed for the diode laser (405 nm) irradiation where the calculated ratio is 0.25:1:0.25 for ITX (0.1%), BAPO (1%), and TPO (1%).

The polymerization kinetics of ESO and LDO were also compared (Figure 5) to a well-known structure largely used in cationic photopolymerization: EPOX. LDO and EPOX

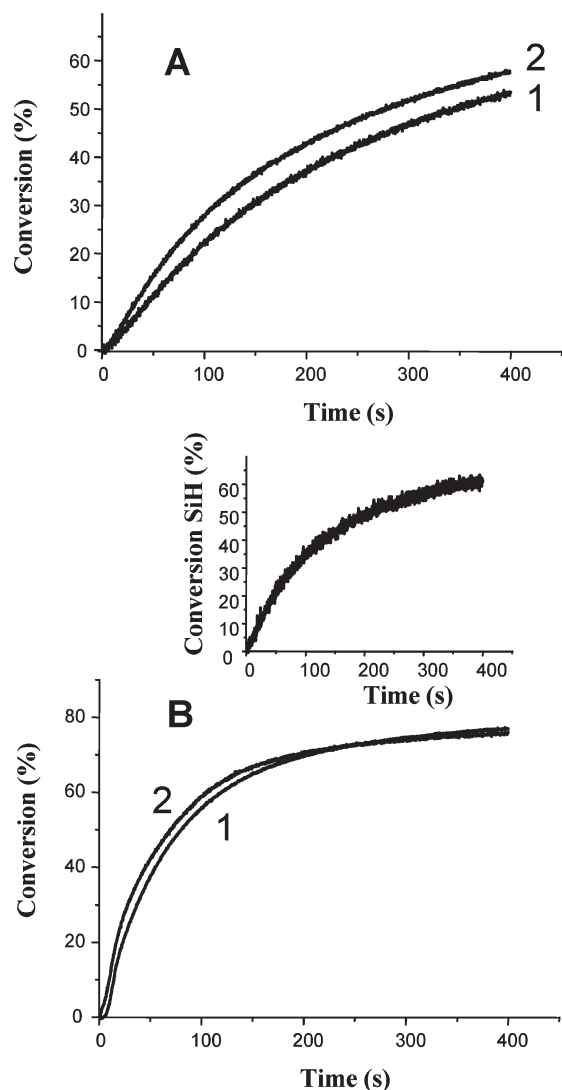


Figure 4. Polymerization profiles of (A) ESO and (B) LDO. Under air. Upon xenon lamp irradiation in the presence of (1) ITX/ Ph_2I^+ (0.1/1% w/w) and (2) ITX/TTMSS/ Ph_2I^+ (0.1/3/1% w/w). Insert: conversion of the Si-H content as a function of time for (2).

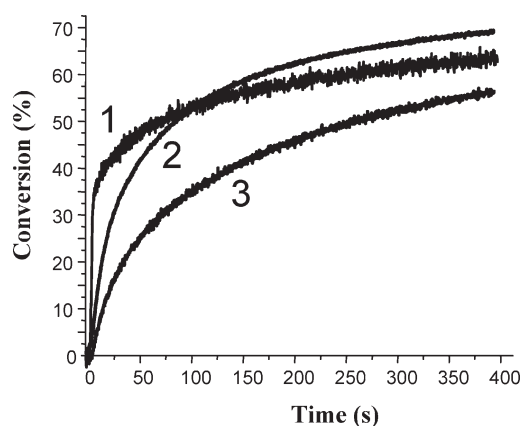


Figure 5. Polymerization profiles of EPOX (1), LDO (2), or ESO (3) under air upon the diode laser irradiation (405 nm) in the presence of the BAPO/TTMSS/ Ph_2I^+ (1/3/1% w/w) photoinitiating system.

are characterized by quite similar polymerization profiles, albeit ESO exhibits a lower reactivity.

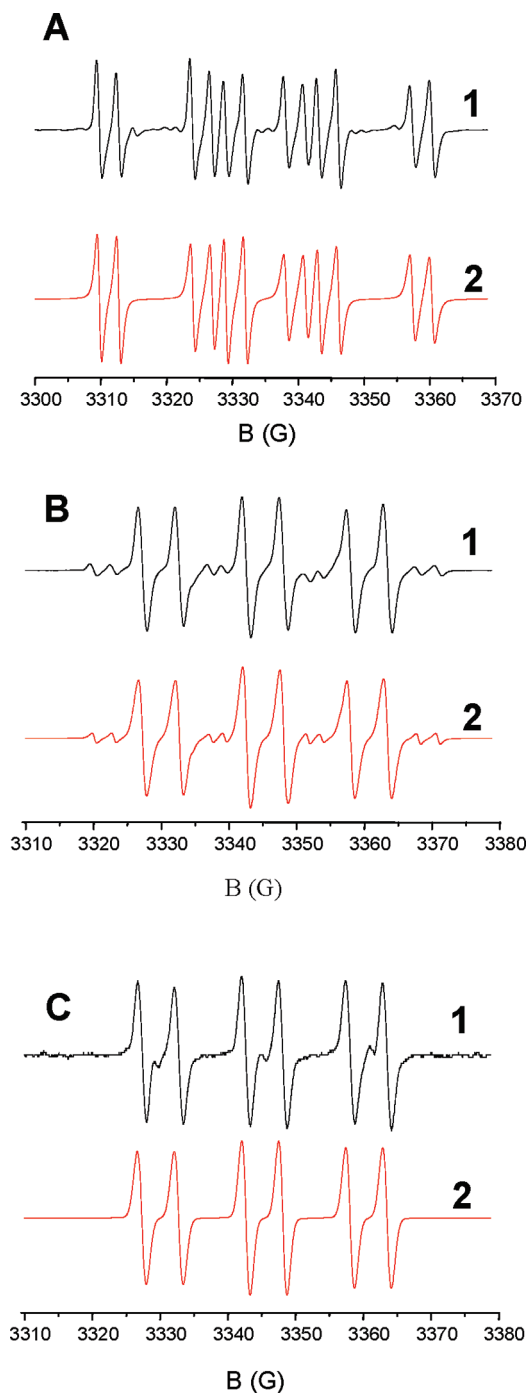
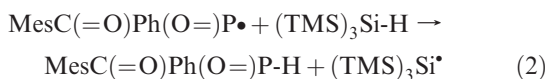
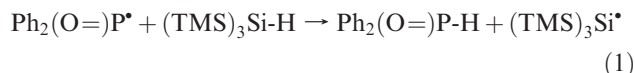


Figure 6. ESR spin trapping spectrum (1) and simulated spectrum (2) obtained by irradiation of (A) TPO, (B) TPO/TTMSS, and (C) BAPO/TTMSS (xenon lamp exposure; PBN 0.05 M). See the text.

All of these experiments show that tack-free uncolored coatings based on renewable cationic monomers can be formed using a FRPCP process, upon low light intensity exposure and under air, even using a less favorable (and by the way less toxic) PF_6^- counteranion instead of SbF_6^- . This can be achieved thanks to the use of the silyl radical chemistry.

2. FRPCP Mechanism. *A. Phosphine-Oxide-Based Systems (TPO; BAPO).* Upon light irradiation of TPO, the phosphinoyl radical generated by homolytic C–P single bond cleavage is clearly observed in ESR-spin trapping experiments (Figure 6A): the hyperfine coupling constants (HFCs) of the phosphinoyl adduct ($a_N = 14.2$; $a_H = 2.9$;

$a_P = 19.2\text{G}$) are in agreement with the literature data¹⁹ Interestingly, in the presence of TTMSS, this phosphinoyl radical is converted into a silyl radical (Figure 6B); the HFCs ($a_N = 15.3$; $a_H = 5.4\text{G}$) are in agreement with the presence of a tris(trimethylsilyl)silyl radical.⁷ This process corresponds to a hydrogen transfer reaction 1. For BAPO, such a reaction 2 is also observed (Figure 6C).



The rate constants of reactions 1 and 2 were determined by LFP through the direct observation of the phosphinoyl radicals of TPO and BAPO at 330 and 450 nm, respectively (Figure 7).²⁰ High rate constants were obtained, that is, 1.4×10^7 and $8.7 \times 10^6 \text{ M}^{-1} \text{ s}^{-1}$ for reactions 1 and 2. The benzoyl counter radicals are not easily observed in ESR-ST or LFP experiments when produced from phosphine oxides. However, when studying another photoinitiator (2,2-dimethoxy-2-phenylacetophenone) that allows the observation of the benzoyl radical in ESR-ST (the dimethoxybenzyl radical also generated is not observed in these ESR-ST experiments),²³ it is worth noting (reaction 3) that silyl radicals are also generated (Figure 3 in the Supporting Information). Therefore, a contribution of the benzoyl radical to the hydrogen abstraction of TPO and BAPO by TTMSS can also con-

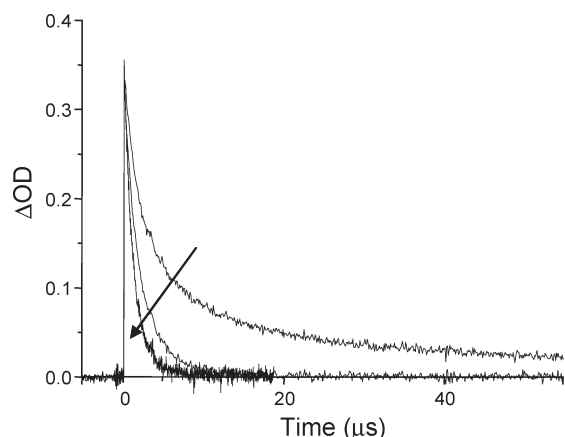
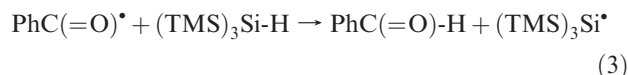


Figure 7. Decay of the TPO phosphinoyl radical observed at 330 nm for different TTMSS concentrations (0; 0.027, and 0.058 M, respectively) in acetonitrile.

tribute to some extent.



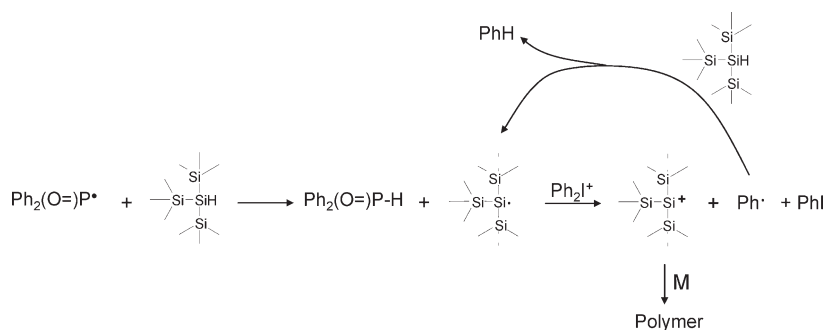
The conversion reactions 1–3 are the key reactions here in the three-component system because the oxidation rate constants of $(\text{TMS})_3\text{Si}^\bullet$ by iodonium salts ($2.6 \times 10^6 \text{ M}^{-1} \text{ s}^{-1}$)⁹ are higher than those obtained in the case of the phosphinoyl radicals generated from TPO and BAPO ($k_{\text{ox}} < 1 \times 10^6 \text{ M}^{-1} \text{ s}^{-1}$) in the formerly designed^{10g} two-component TPO/ Ph_2I^+ system. Therefore, the main interest of the TTMSS addition is the formation of radicals that can be more easily oxidized, the resulting silylium cations being excellent polymerization initiating structures, as already noted in other systems, for example, camphorquinone/iodonium salt/TTMSS.⁹

Interestingly, keeping in mind that the initial Si–H content is much higher than the TPO or BAPO content, the high conversion of the Si–H functions observed above ($\sim 70\%$) demonstrates that TTMSS reacts not only with the phosphinoyl or the benzoyl radical but also with the phenyl radical generated from the reduction of Ph_2I^+ (Scheme 2).

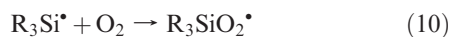
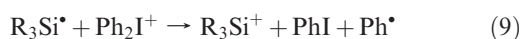
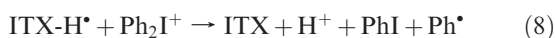
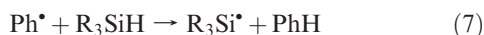
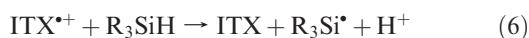
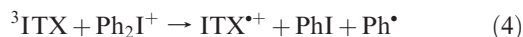
Kinetic considerations can be made by taking into account the various interaction rate constants (k_{int}) determined in acetonitrile and the diffusion rate constants (k_{diff}) calculated in the monomer media. The viscosities of these monomers are 450, 10, and 250 cP for ESO, LDO, and EPOX, respectively. The corresponding k_{diff} values were calculated according to the classical Stokes–Einstein equation: 1.3×10^7 ; 5.9×10^8 , and $2.4 \times 10^7 \text{ M}^{-1} \text{ s}^{-1}$ for ESO, LDO, and EPOX, respectively. As a consequence, the k_{int} values measured in solution and found lower than k_{diff} values will be used in the monomer media; if not, they will be leveled off at the k_{diff} value. It is clearly found that phosphinoyl radicals preferentially react with TTMSS than with oxygen ($k_{1-2}[\text{TTMSS}] \gg k_{\text{O}_2}[\text{O}_2]$: 1.3×10^6 vs $2.6 \times 10^4 \text{ s}^{-1}$ in ESO). The interaction of the phosphinoyls with the monomers can probably be neglected ($k < 10^6 \text{ M}^{-1} \text{ s}^{-1}$). All of these data evidence that the conversion of phosphinoyls to silyls (1–2) is probably the key pathway.

B. ITX-Based System. The addition of TTMSS to ITX/ Ph_2I^+ leads to an only small increase in the polymerization rates. However, a quite high Si–H conversion is found ($\sim 70\%$). This demonstrates that a hydrogen abstraction process occurs. As already suggested in ref 9 and taking the ITX/ Ph_2I^+ and radical/ Ph_2I^+ interactions previously discussed,^{1,2} a plausible general mechanism (reactions 4–10) should involve: (i) an efficient electron transfer process in $^3\text{ITX}/\text{Ph}_2\text{I}^+$ (reaction 4), which promotes the decomposition of the iodonium salt^{1,2,9} with a high rate constant

Scheme 2



($k = 9.6 \times 10^9 \text{ M}^{-1} \text{ s}^{-1}$),⁹⁽ⁱⁱ⁾ a strong $^3\text{ITX}/\text{R}_3\text{SiH}$ interaction (reaction 5) ($k = 4.1 \times 10^7 \text{ M}^{-1} \text{ s}^{-1}$) associated with a high ketyl radical quantum yield ($\Phi_K = 0.7^{21}$), (iii) an inefficient monomer quenching ($k < 10^6 \text{ M}^{-1} \text{ s}^{-1}$), and (iv) a reaction of ITX^{*+} (reaction 6) and the phenyl radical (reaction 7) with the silane.⁹ Other processes (reactions 8–10) can also be invoked for the formation of the cationic species.⁹



The $^3\text{ITX}/\text{Ph}_2\text{I}^+$ reaction pathway being already highly efficient and leading to the formation of initiating cationic species (reaction 4), the addition of TTMSS does not improve the process drastically. However, the $^3\text{ITX}/\text{R}_3\text{SiH}$, $\text{ITX}^{*+}/\text{R}_3\text{SiH}$, and $\text{Ph}^\bullet/\text{R}_3\text{SiH}$ interactions explain the high Si–H conversion found in Figure 4. Indeed, from kinetic grounds, ^3ITX preferentially reacts with TTMSS rather than with Ph_2I^+ ($k_5 [\text{TTMSS}] \gg k_4 [\text{Ph}_2\text{I}^+]$: 1.7×10^6 vs $5.5 \times 10^5 \text{ s}^{-1}$ in ESO). However, keeping in mind that the initial Si–H content is higher than the ITX content, the high conversion of the Si–H functions observed in Figure 4 (~70%) demonstrates that TTMS not only reacts with ^3ITX but also with derived intermediates (Ph^\bullet , ITX^{*+}), in agreement with the presence of reactions 6 and 7.

For the $\text{ITX}/\text{TTMSS}/\text{Ph}_2\text{I}^+$ system, the cationic initiating species are formed in reactions 4, 6, 8, 9, and 10, and 10', and the high silane conversion clearly indicates an important pathway for the silyl radicals formation in reactions 5–7; because reaction 9 is more efficient than reaction 10 ($k_9 [\text{Ph}_2\text{I}^+] > k_{10} [\text{O}_2]$: 5.9×10^4 vs $3 \times 10^4 \text{ s}^{-1}$) in ESO the silylium cation (R_3Si^+) is presumably one of the preferentially initiating structure. The H^+ and R_3SiO_2^+ cationic species generated from reactions 6, 8, and 10' should also contribute to some extent. Reactions 6 and 8 are very usual. In a recent paper,⁹ R_3SiO_2^+ was shown to be an important initiating species in the FRPCP of the less viscous EPOX monomer, where $k_9 [\text{Ph}_2\text{I}^+] < k_{10} [\text{O}_2]$: 5.9×10^4 versus $9 \times 10^4 \text{ s}^{-1}$.

The ability of the silylium cation (R_3Si^+) to initiate a cationic polymerization is also supported here using molecular orbital calculations.²² Two model epoxides were considered: 1,2-epoxypropane (EP) and cyclohexene oxide (CHO). The epoxy ring-opening reaction by $(\text{TMS}_3\text{Si})^+$ is found to be highly exothermic, that is, -135 and -152 kJ/mol for EP and CHO, respectively (Figure 8). This strong

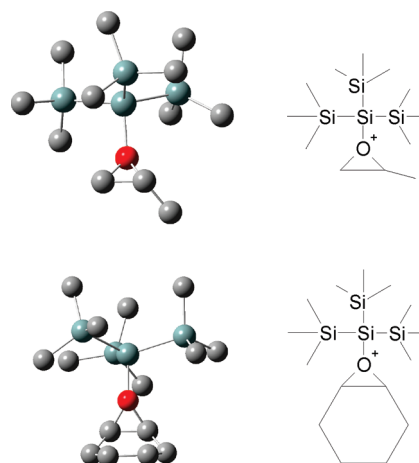


Figure 8. Structures optimized at UB3LYP/6-31+G* level for the adduct of $(\text{TMS}_3\text{Si})^+$ to a model epoxy. The hydrogen atoms are not depicted.

interaction is in full agreement with the excellent efficiency obtained for the new proposed systems.

Conclusions

In the present article, new systems based on the silyl radical chemistry are proposed for the photoinitiation of the cationic polymerization of ESO and LDO as renewable monomers. An excellent efficiency is found for the first time upon solar irradiation and under air. This contribution obviously parallels other studies on the development of green chemistry in radiation curing, the fundamental striking difference here being the possibility to work under sunlight in films in contact with the atmosphere and to get uncolored tack-free coatings. In the cationic photopolymerization area, this could open up new ideas of applications that should have to be carried out under air using near-UV or visible wavelengths (from lamps, LED, or sun) and very low light intensities.

Supporting Information Available: Polymerization profiles of LDO under air for Xenon lamp irradiation and diode laser irradiation, emission spectrum for the xenon lamp and absorption coefficients for ITX, BAPO, and TPO in acetonitrile, and ESR spin trapping spectrum obtained by irradiation with a Xe-Hg lamp of 2,2-dimethoxy-2-phenylacetophenone with TTMSS. This material is available free of charge via the Internet at <http://pubs.acs.org>.

References and Notes

- (1) (a) Crivello, J. V. *Photoinitiators for Free Radical, Cationic, and Anionic Photopolymerization*, 2nd ed.; Bradley, G., Ed.; New York, 1998. (b) Crivello, J. V. *Ring-Opening Polymerization*, Brunelle, D. J., Ed.; Hanser Publishers: Munich, 1993. (c) Fouassier, J. P. *Photoinitiation, Photopolymerization and Photocuring: Fundamental and Applications*; Hanser Publishers: New York, 1995. (d) *Photochemistry and UV Curing*; Fouassier, J. P., Ed.; Research Signpost: Trivandrum, India, 2006.
- (2) (a) Fouassier, J. P. In *Radiation Curing in Polymer Science and Technology*; Fouassier, J. P., Rabek, J. F., Eds.; Elsevier Science Publishers: London, 1993. (b) Tehfe, M. A.; Lalevée, J.; Allonas, X.; Fouassier, J. P. *Macromolecules* **2009**, *22*, 8669–8674.
- (3) Crivello, J. V. *Chem. Mater.* **1992**, *4*, 692–699.
- (4) Chakrapany, S.; Crivello, J. V. *J. Macromol. Sci., Pure Appl. Chem.* **1998**, *A35*, 691–710.
- (5) Ortiz, R. A.; Lopez, D. P.; de Lourdes Guillen Cisneros, M.; Valverde, J. C. R.; Crivello, J. V. *Polymer* **2005**, *46*, 1535–1541.
- (6) (a) Crivello, J. V. *J. Macromol. Sci. Part A* **2009**, *46*, 474–483. (b) Crivello, J. V.; Bulut, U. *J. Polym. Sci., Part A: Polym. Chem.* **2005**, *43*, 5217–5231.

- (7) Lalevée, J.; Blanchard, N.; El-Roz, M.; Graff, B.; Allonas, X.; Fouassier, J. P. *Macromolecules* **2008**, *41*, 4180–4186.
- (8) (a) Lalevée, J.; Dirani, A.; El-Roz, M.; Allonas, X.; Fouassier, J. P. *J. Polym. Sci., Part A: Polym. Chem.* **2008**, *46*, 3042–3047. (b) Lalevée, J.; Allonas, X.; Fouassier, J. P. *Chem. Phys. Lett.* **2009**, *469*, 298–303.
- (9) Lalevée, J.; El-Roz, M.; Allonas, X.; Fouassier, J. P. *J. Polym. Sci., Part A: Polym. Chem.* **2008**, *46*, 2008–2014.
- (10) (a) Ledwith, A. *Polymer* **1978**, *19*, 1217–1219. (b) Baumann, H.; Timpe, H. J. *Z. Chem.* **1984**, *24*, 18–19. (c) Yagci, Y.; Ledwith, A. *J. Polym. Sci., Part A: Polym. Chem.* **1988**, *26*, 1911–1918. (d) Yagci, Y.; Kminek, I.; Schnabel, W. *Polymer* **1993**, *34*, 426–428. (e) Bi, Y.; Neckers, D. C. *Macromolecules* **1994**, *27*, 3683–3693. (f) Dursun, C.; Degirmenci, M.; Yagci, Y.; Jockusch, S.; Turro, N. J. *Polymer* **2003**, *44*, 7389–7396. (g) Yagci, Y.; Schnabel, W. *Makromol. Chem. Rapid Commun.* **1987**, *8*, 209–213.
- (11) Crivello, J. V.; Sangermano, M. *J. Polym. Sci., Part A: Polym. Chem.* **2001**, *39*, 343–356.
- (12) (a) Yagci, Y.; Pappas, S. P.; Schnabel, W. *Z. Naturforsch.* **1987**, *42A*, 1425–1428. (b) Arsu, N.; Hizai, G.; Yagci, Y. *Macromol. Reports* **1995**, 1257–1262. (c) Yagci, Y.; Reetz, I. *Prog. Polym. Sci.* **1998**, *23*, 1485–1538.
- (13) Degirmenci, M.; Onen, A.; Yagci, Y.; Pappas, S. P. *Polym. Bull.* **2001**, *46*, 443–449.
- (14) Crivello, J. V. *J. Polym. Sci., Part A: Polym. Chem.* **2009**, *47*, 866–875.
- (15) Crivello, J. V.; Liu, S. S. *Chem. Mater.* **1998**, *10*, 3724–3731.
- (16) Durmaz, Y. Y.; Moszner, N.; Yagci, Y. *Macromolecules* **2008**, *41*, 6714–6718.
- (17) Lalevée, J.; Allonas, X.; Fouassier, J. P. *J. Am. Chem. Soc.* **2002**, *124*, 9613–9621.
- (18) Tordo, P. Spin-Trapping: Recent Developments and Applications. In *Electron Spin Resonance*; Atherton, N. M.; Davies, M. J.; Gilbert, B. C., Eds.; The Royal Society Of Chemistry: Cambridge, U.K., 1998; Vol. 16.
- (19) Brunton, G.; Gilbert, B. C.; Mawby, R. J. *J. Chem. Soc., Perkin Trans. II* **1976**, 650.
- (20) (a) Sluggett, G. W.; McGarry, P. F.; Koptuyg, I. V.; Turro, N. J. *J. Am. Chem. Soc.* **1996**, *118*, 7367–7372. (b) Jockusch, S.; Landis, M. S.; Freiermuth, B.; Turro, N. J. *Macromolecules* **2001**, *34*, 1619–1626.
- (21) Lalevée, J.; Dirani, A.; El-Roz, M.; Allonas, X.; Fouassier *Macromolecules* **2008**, *41*, 2003–2010.
- (22) (a) Frisch, M. J.; Trucks, G. W.; Schlegel, H. B.; Scuseria, G. E.; Robb, M. A.; Cheeseman, J. R.; Zakrzewski, V. G.; Montgomery, J. A., Jr.; Stratmann, R. E.; Burant, J. C.; Dapprich, S.; Millam, J. M.; Daniels, A. D.; Kudin, K. N.; Strain, M. C.; Farkas, O.; Tomasi, J.; Barone, V.; Cossi, M.; Cammi, R.; Mennucci, B.; Pomelli, C.; Adamo, C.; Clifford, S.; Ochterski, J.; Petersson, G. A.; Ayala, P. Y.; Cui, Q.; Morokuma, K.; Salvador, P.; Dannenberg, J. J.; Malick, D. K.; Rabuck, A. D.; Raghavachari, K.; Foresman, J. B.; Cioslowski, J.; Ortiz, J. V.; Baboul, A. G.; Stefanov, B. B.; Liu, G.; Liashenko, A.; Piskorz, P.; Komaromi, I.; Gomperts, R.; Martin, R. L.; Fox, D. J.; Keith, T.; Al-Laham, M. A.; Peng, C. Y.; Nanayakkara, A.; Challacombe, M.; Gill, P. M. W.; Johnson, B. G.; Chen, W.; Wong, M. W.; Andres, J. L.; Gonzalez, C.; Head-Gordon, M.; Replogle, E. S.; Pople, J. A. *Gaussian 98*, revision A.11; Gaussian, Inc.: Pittsburgh, PA, 2001. (b) Foresman, J. B.; Frisch, A. In *Exploring Chemistry with Electronic Structure Methods*, 2nd ed.; Gaussian, Inc.: Pittsburgh, PA, 1996.
- (23) Criquei, A.; Lalevée, J.; Allonas, X.; Fouassier, J. P. *Macromol. Chem. Phys.* **2008**, *209*, 2223–2231.